

Experimental Study of the Compression Response of Fluted-Core Composite Panels with Joints

Marc R. Schultz¹ and Cheryl A. Rose²

NASA Langley Research Center, Hampton, VA 23681-2199, USA

J. Carlos Guzman³ and Douglas McCarville⁴

The Boeing Company, Seattle, WA 98124-2207, USA

and

Mark W. Hilburger²

NASA Langley Research Center, Hampton, VA 23681-2199, USA

Fluted-core sandwich composites consist of integral angled web members spaced between laminate face sheets, and may have the potential to provide benefits over traditional sandwich composites for certain aerospace applications. However, fabrication of large autoclave-cured fluted-core cylindrical shells with existing autoclaves will require that the shells be fabricated in segments, and joined longitudinally to form a complete barrel. Two different longitudinal fluted-core joint designs were considered experimentally in this study. In particular, jointed fluted-core-composite panels were tested in longitudinal compression because longitudinal compression is the primary loading condition in dry launch-vehicle barrel sections. One of the joint designs performed well in comparison with unjointed test articles, and the other joint design failed at loads approximately 14% lower than unjointed test articles. The compression-after-impact (CAI) performance of jointed fluted-core composites was also investigated by testing test articles that had been subjected to 6 ft-lb impacts. It was found that such impacts reduced the load-carrying capability by 9% to 40%. This reduction is dependent on the joint concept, component flute size, and facesheet thickness.

I. Introduction

In recent years, fiber-reinforced composite structures have become more accepted for many different applications, including aerospace vehicles. When properly applied, composite structures can have many benefits over traditional metallic structures, including lower mass, better fatigue resistance, lower part count, and reduced life-cycle cost. During NASA's recent efforts to develop new launch vehicles, composite materials were considered and baselined for studies of a number of structures. Specifically, several of the primary dry shell components such as interstages, shrouds, and frustums were baselined as composite (see, for example, refs. 1-4). Various shell designs and construction methods were considered, including several composite sandwich shells. Because they possess a low-density core and a high bending stiffness, composite sandwich shells can be structurally efficient for applications where the structure is prone to buckling or requires high bending stiffness. Traditional composite sandwich panels are composed of inner and outer facesheets separated by a core material such as polymer foam,

¹ Research Aerospace Engineer, Structural Mechanics and Concepts Branch, Mail Stop 190, AIAA Senior Member, marc.r.schultz@nasa.gov.

² Senior Research Aerospace Engineer, Structural Mechanics and Concepts Branch, Mail Stop 190, AIAA Senior Member.

³ Manufacturing Research and Development Engineer, Boeing Research & Technology, P.O. Box 3707, Mail Stop 4R-05.

⁴ Manufacturing Research and Development Technical Fellow, Boeing Research & Technology, P.O. Box 3707, Mail Stop 4R-05.

balsa wood, or aluminum or aramid/phenolic honeycomb. The facesheets and core are typically joined with film adhesive in either a co-cure (with green facesheets) or a hot-bond (with pre-cured facesheets) operation. Once joined, the facesheets carry tension and compression loads, and the core keeps the facesheets separated while carrying the through-thickness shear loads. Though structurally efficient, traditional composite sandwich structures can have manufacturing and in-service drawbacks such as poor facesheet-to-core bond, reduced facesheet properties, and moisture absorption in the core.^{5,6} To address some of these shortcomings, alternative sandwich-type structural concepts are being developed. One such structural concept is manifested in *fluted-core* composite structures (sandwich structures that consist of integral angled web members and structural radius fillers spaced between laminate face sheets, see Fig. 1 and Ref. 5). Launch-vehicle cylindrical shell structures can have diameters as large as 33 ft, and cannot be autoclave cured as a unitized barrel in existing autoclave facilities. Because of the associated costs of building and operating new autoclaves, longitudinal joints will be required if sections of the barrels are to be autoclave cured. That is, it is proposed that such large cylinders can be fabricated by first building autoclave-cured panels and then assembling them into a complete barrel using longitudinal joints.

The primary loading condition in dry launch-vehicle cylindrical-shell sections is longitudinal compression. An experimental study to better understand the compression behavior and failure modes of fluted-core composite structures with longitudinal joints is detailed herein. Two different fluted-core composite joint designs were considered. Test articles representing both joint designs were tested in pristine and impact-damaged states. Impacted test articles were tested to provide preliminary data on the impact damage resistance and tolerance of fluted-core composite joints.

A brief discussion of sandwich composite joints and the particular joints to be examined in the present paper is provided in Section II. Descriptions of the test articles are given in Section III, and representative experimental results are given and discussed in Section IV. Closing remarks are provided in Section V.

II. Sandwich Composite Joints

Many joint designs for composite sandwich structures consist of large, often metallic, splice plates that are bolted, bonded, or bolted and bonded across the joint. In addition, densification of the core in the region of the joint is often necessary. These joint designs can add significant weight to an otherwise lightweight structure. Additionally, the added stiffness of the splice plates and the densification will draw more load into the joint region and can reduce the buckling performance and structural efficiency of the structure. Another typical sandwich-composite joint design has the cores tapered to solid laminates and splice plates bolting the butted solid laminates. These joints can be particularly problematic in buckling- or stiffness-critical structures because not only is more load drawn into the joint, but the bending stiffness is significantly reduced. (For a discussion of some of these joint issues for welded orthogrid metallic structures, see Ref. 7.)

The fluted-core composite panels considered herein were produced by Boeing and were joined using two types of scarf joints, as shown in Fig. 2. In both joint designs, adjacent shell sections are butted together, the facesheets are scarfed, and similar scarf planks are bonded over the scarfed region. The first joint design, herein termed the *basic* joint, consists of only the scarfed shells, adhesive, and the scarf planks. The second joint design, herein termed the *I-beam* joint, is similar but has the addition of a perpendicular web and noodles between the two separate panels. Potential advantages of these joint designs are that they add very little additional weight to the structure, they are close to stiffness neutral in relation to the surrounding structure, and they can be applied in an out-of-autoclave process. The I-beam joint was explored because it allows for more variation in how the panels of a closed shell fit together; that is, the flanges on the I-beam can be sized as needed to fill the gap between the outermost noodles of the separate panels. For both joint types, the scarf plank was 4.5-in. wide with a 1.5-in.-wide flat region. The joint width was sized primarily by the face-sheet thickness, and the conservative taper ratio of 0.3-in. per ply.

III. Test Article Description

The objective of the experimental effort described herein is to investigate localized compression failures of fluted-core composite panels with longitudinal scarf joints. The test articles were designed so that they would fail in compression without large global out-of-plane deformations. Test articles with both of the two joint designs were tested in pristine and impact-damaged states.

The fluted-core composite cross section that was used in this study was termed the *subscale* cross section in Ref. 5, and the test-article geometries were similar to those in Ref. 5. The test articles were 0.74-in. thick and consisted of five flutes (not including the joint). All test articles were fabricated by wrapping unidirectional 350-°F toughened carbon-epoxy prepreg plies around trapezoidal mandrels, arranging the wrapped mandrels with pultruded unidirectional-prepreg radius fillers (noodles), and placing prepreg facesheets above and below the wrapped

mandrels. The entire arrangement was then autoclave co-cured and the mandrels were removed after cure. The total web layup was $[\pm 45/\pm 45]_T$ (where the “T” subscript denotes total layup) and the total facesheet layup (including the plies originally wrapped around the mandrels) was $[\pm 45/0/90]_S$. (Note: The right-handed coordinate systems for describing the layouts have the 0-degree direction as the longitudinal test-article direction, the 90-degree direction as in plane and perpendicular to the 0-degree direction, and the normals as shown by the red arrows in Fig. 1.) To make a jointed test article, a cut was made down the middle of a flute, the facesheets were scarfed, and then the scarf planks were applied. The scarf planks were bonded to the scarfed panels using 0.015-in.-thick 250-°F-cure film adhesive under autoclave heating and pressure. Though the considered test-article joints were manufactured using an autoclave, it is possible using simple tooling to apply the same temperatures and pressures in an out-of-autoclave process.

The test articles had a total length of 11 in. with 1.5-in.-long by 0.125-in.-thick G-10 fiberglass tabs applied to both faces at each end. These tabs had a 45-degree bevel that tapered down to the test article and are shown in Fig. 3. Additionally, a 1-in.-long section on both ends of the test articles was potted into a steel frame using an epoxy grout. Considering the tabs and potting, the test length of the subscale test articles was 8 in. The test articles with the basic joint were approximately 5.75-in. wide on the wide face and 5.25-in. wide on the narrow face. The test articles with the I-beam joint were approximately 6.25-in. wide on the wide face and 5.75-in. wide on the narrow face. As shown in Figs. 2a and 2c, for both types of test articles, the wide face was termed the *front* and the narrow face was termed the *back*. To prepare the test articles for testing, all edges were machined flat and parallel, or flat and perpendicular. Half of the test articles of each joint type were tested in a pristine condition and half were tested after being subjected to a 6 ft-lb impact from a ½-in.-diameter spherical indenter.

Each test article had electrical-resistance strain gages applied at 8 locations located 0.5 in. above the lower tabs. Further, they were painted with a black-and-white speckle pattern to enable full-field optical displacement and strain measurements using the video image correlation system VIC-3D.⁸ The test articles were tested in a hydraulic load frame with a constant cross-head rate of 0.005 in./min, and four direct-current displacement transducers (DCDTs) were used to measure relative platen displacement and rotation. To help ensure that the test articles were primarily loaded in longitudinal compression, one of the loading platens was mounted on a screw-adjustable pivot. Despite these precautions, some measurable rotation of the loading platen occurred during some of the tests. This imparted a slight amount of bending in some of the test articles. However, these rotations accounted for less than 1.5% of the strain in all the test articles so it is believed that these rotations were insignificant for the results in all cases.

IV. Experimental Results and Discussion

A. Summary of Results of Unjointed Test Articles

The behavior of the unjointed test articles that was presented in Ref. 5 is briefly reviewed here as a baseline with which to compare the jointed test articles. The experimental results for pristine and impacted unjointed and basic-joint test articles are summarized in Table 1. Two unjointed pristine test articles (designated CPA-1B and CPA-2B) were tested and the average results are shown in Table 1. For these test articles, the first out-of-plane deformations seen were inward facing dimples (single out-of-plane half waves) in each of the long spans (see Fig. 1a) adjacent to both the top and bottom tabs. As the loading was continued, these dimples developed into distributed buckling patterns with 9 half waves along the length of the test article in each of the long spans, as seen in Figs. 4a and b. For each pristine test article, loading was continued up to a peak load between 51,000 and 54,000 lb at which point the test article underwent a sudden transverse failure across the entire cross section. Two impacted test articles were loaded in compression after being subjected to 6 ft-lb impacts from a ½-in.-diameter spherical indenter; one test article (designated CPA-1A) was impacted over the central short span in the back face (see Fig. 1a) and the other (designated CPA-2A) was impacted over one of the central noodles on the back face as shown in Table 1. The short-span impact caused significant rupturing of the facesheet and a near-complete penetration. As identified by ultrasonic scans, the damage zone was limited by the adjacent noodles, but extended within the impacted short span. The over-noodle impact caused a residual dent with a depth of 0.022 in., no visible facesheet rupture, and a damage zone that extended along the noodle. For both impact types, delamination in the faces was clear in the ultrasonic scans, but it was difficult to ascertain the extent of damage, if any, within the noodles. During loading, both impacted test articles developed long-span dimples near the tabs, similar to those in the pristine test articles, and the inward deflection of the impact damaged area increased with increasing load. Additionally, as the loading continued, buckling patterns with 7 or 9 halfwaves along the test-article length developed in most of the long spans. Despite the differences in the impact location, both impacted unjointed test articles failed at similar loads between 30,000 lb and 32,000 lb. The average longitudinal stiffnesses of the pristine and impacted test articles were 613 and 605 kips/in., respectively. These stiffnesses were calculated from the load vs. displacement data for loads between 10 and 30 kips

because this load range is high enough that it is past initial nonlinearities due to test-article settling and low enough that the local buckling has not yet occurred. Each pristine unjointed test article had 30 strain gages on the faces and each impacted unjointed test article had 27 strain gages on the faces. The average strain in these strain gages at failure was 7,300 $\mu\epsilon$ for the pristine test articles, and 4,500 $\mu\epsilon$ and 4,600 $\mu\epsilon$ for the impacted test articles. Taking the average of all the gages seems to give a reasonable effective strain at failure that can be used as a relative measure with which to compare the performance of different test-article configurations.

B. Test Articles with Basic Joint

Two test articles with the basic joint were tested. One was tested in the pristine condition and one was tested after impact. The results of the basic-joint tests are summarized in Table 1. Based on the load vs. displacement data for loads between 10 and 30 kips, the two basic-joint test articles were, on average, about 11% stiffer than the unjointed test articles; this increase in stiffness resulted from the additional material in the scarf region of these test articles. Each basic-joint test article had 6 strain gages on the faces 1 in. above the bottom potting.

1. Pristine Basic-Joint Test Article

The pristine basic-joint test article was designated CJA-3B. The overall response of the basic-joint test article was similar to the response of the unjointed test articles. During the initial stage of loading, inward-facing dimples (single out-of-plane half waves) formed in both of the long spans faces on the back face adjacent to both the top and bottom tabs. A longitudinally aligned outwardly displaced ridge also developed on the back face along the center of the test article, which was also the center of the joint (Fig. 5a). On the front face, dimples developed in the three flutes with long spans, including the flute with the joint line. As the loading continued, additional half waves developed on both faces along the lengths of each of the flute long spans. Like the unjointed test articles, nine half waves developed along the length of each long span on both the front and back faces. At a load of 58,500 lb, an event occurred where there was a jump in strains at several of the strain gages, but with no drop in load. Loading continued monotonically until a load of 59,200 lb. The out-of-plane deformations at this peak load are shown in Fig. 5. The amplitude of the inward and outward half-wave deflections was the largest in the rightmost flute of the front face of the test article, having maximum deflection of approximately 0.025 in. inward and outward (Fig. 5b). Failure occurred as a sudden transverse failure across the entire test-article width. Both scarf planks failed along with the rest of the test article. The material failure occurred through outward half waves on both the front and back faces. The stiffness of the pristine basic-joint test article was 12% greater and the failure load was 13% higher than the average of those for the pristine unjointed test articles. However, because of softening behavior seen over the entire load range, the average strains showed a larger discrepancy—the average strain from the 6 strain gages at failure was 8,900 $\mu\epsilon$, which is 22% higher than the average failure strain of the pristine unjointed test articles.

2. Impacted Basic-Joint Test Article

The impacted basic-joint test article was designated CJA-3A. This test article was impacted with a ½-in. spherical tup with a 6 ft-lb impact energy. The impact location was over the splice plate and over a noodle on the back face (Table 1). Impact damage included a residual dent with a depth of 0.007-in., but no visible cracks, tears, or ruptures. An ultrasonic scan of the impact damage showed a damage zone that extended along the noodle (see Fig. 6). The impact damage in this basic-joint test article was less extensive than the impact damage in the baseline unjointed test article that was impacted in the same location.

As the impacted basic-joint test article was loaded, the initial response was similar to that of the pristine basic-joint test article. That is, this test article was 11% stiffer than the average of the impacted unjointed test articles and, during the initial stage of loading, inward-facing dimples formed on both faces of the panel at both ends of each long span near the fiberglass tabs. As the loading continued, outward-facing ridges developed along the joint line on both faces of the test article. Additionally, smaller ridges developed in the long spans of both outer flutes on the front face (Fig. 7b). Initially, the impact damage area was dented inward. However, as the loading continued further, the impact damage area “popped” through to an outward deflection starting with a discrete event that included a shape change at 27,500 lb. Another discrete event occurred at 29,300 lb. This out-of-plane deformation in the impact damage area was the largest in the test article, with a maximum value of 0.04 in. (Fig. 7) just prior to ultimate failure of the test article. At a load of 35,800 lb, there was a sudden transverse failure across the test article through the impact damage area. This failure load is 40% lower than that of the pristine test article, but 14% higher than the average failure loads of the impacted unjointed test articles. On the front face, the scarf plank buckled outward, but did not rupture; the failure ran under the scarf plank. That is, the scarf plank delaminated presumably along the adhesive line. The scarf plank on the back face ruptured along with the rest of the back face. The average strain from

the 6 strain gages just prior to failure was $5,100 \mu\epsilon$, which is 43% lower than that of the pristine test article, but 12% higher than the average failure strains of the impacted unjointed test articles.

C. Test Articles with I-Beam Joint

Four test articles with the I-beam joint were tested. Two were tested in the pristine condition and two were tested after impact. The results of the I-beam-joint tests are summarized in Table 2. On average, for loads between 10 and 30 kips, the four I-beam-joint test articles were approximately 22% stiffer than the unjointed test articles. However, if the larger width of the I-beam-joint test articles is taken into account, these test articles were only about 12% stiffer than the unjointed test articles. Each I-beam-joint test article had 6 strain gages on the faces 1 in. above the bottom potting.

1. Pristine I-Beam-Joint Test Articles

The two pristine I-beam-joint test articles were designated CJA-2B and CWA-1B. As CJA-2B was loaded, there was some global panel bending toward the back face of the test article. Inward dimples developed adjacent to the tabs in the two long spans on the back face, and in the two outer long spans on the front face (Fig. 8). Distributed buckling was not observed along the length of any of the flutes. At 42,300 lb, a sudden transverse failure occurred through both faces of the test article about 1.8 in. from the bottom tabs. In the joint region of the front face, the scarf plank separated from the underlying structure and the scarf plank bowed outward. On the back face, the material failure passed through both the scarf plank and the underlying structure. The out-of-plane deformations just prior to failure are shown in Fig. 8.

Slight global panel bending toward the back face occurred as CWA-1B was loaded. During initial loading, inward facing half waves developed near the tabs in all of the long spans on both the front and back faces (two flutes on each face). With continued loading, distributed buckling with 9 half waves developed along the length of the two long front spans. No distributed buckling was seen on the back of the test article. As the loading continued, at 47,400 lb, a single large bulge developed suddenly directly over the I-beam about 1.9 in. below the upper tab on both the front and back faces, i.e., both faces bulged outward at essentially the same location. The bulge on the front surface had a maximum outward displacement of about 0.1 in. relative to the displacement of the surrounding face, and the bulge on the back face had a much smaller maximum outward displacement of about 0.02 in. relative to the displacement of the surrounding face. Additionally, the bulge on the front surface was much more localized and had smaller in-plane dimensions than the back-surface bulge (Fig. 9). It is speculated that these bulges were caused by a separation of the scarf plank on the front face from the underlying joint structure, and that this failure also allowed the back face, and web, to bulge out in the opposite direction. After the bulges appeared, the load continued to increase to a peak load of 47,600 lb, at which point there was a 600-lb drop in load. After the load drop, the load again increased until there was a sudden transverse failure through the bulges at a load of 47,400 lb. On the front face, the scarf plank did not rupture, but bowed out over its entire width, and the material failed in the structure beneath the scarf plank. On the back face, the entire face, including the scarf plank, failed. The out-of-plane deformations just prior to failure are shown in Fig. 9.

Test article CJA-2B failed at a load about 11% lower than test article CWA-1B, and the average failure load for the two test articles was 45,000 lb. This average failure load is 24% lower than the failure load of the pristine basic-joint test article, and 14% lower than the average failure load of the pristine unjointed test articles. Similarly, the average failure strain for test article CJA-2B was 9% lower than that for test article CWA-1B, and the average failure strain for the two test articles was $6,200 \mu\epsilon$. This average failure strain was 29% lower than the average failure strain of the pristine basic-joint test article, and 15% lower than the average failure strain of the pristine unjointed test articles.

2. Impacted I-Beam-Joint Test Articles

The two impacted I-beam-joint test articles were designated CJA-2A and CWA-1A. As shown in Table 2, test article CJA-2A was impacted on the back face in the span separating the I-beam from an adjacent noodle, and test article CWA-1A was impacted in the middle of the back face directly over the I-beam. Impact damage on CJA-2A included a residual dent with a 0.015-in. dent depth and a semi-circular tear in the facesheet at the impact site. In addition, as seen in the ultrasonic scan of Fig. 10a, the over-span impact resulted in a damage zone that extended along the length of the test article, parallel to the noodles. The majority of the damage was limited to the area between the adjacent noodles, but there was some delamination damage in the facesheets over the noodles. The extent of damage in this case was slightly larger than in the corresponding unjointed test article that was impacted over the central short span in the back face. The impact damage in CWA-1A included a residual dent with a dent depth of 0.010 in., but no visible cracks, tears, or ruptures in the facesheet and a damage zone that extended along

the noodle (see Fig. 10b). The damage zone in this case was larger than for the basic-joint test article that was impacted over the noodle.

As CJA-2A was loaded, there was some global panel bending toward the back face. As the loading continued, single inward-facing dimples developed adjacent to the tabs in all of the long spans on both faces. The impact-damaged area initially deformed inward. At 24,000 lb, a small pop was heard, and in discrete events at 37,200 lb and at 39,300 lb, two outward-facing bumps formed adjacent to the impact-damaged area (Fig. 11). These bumps appear to have developed because of localized delamination or localized failure of the joint bond. No discrete events were observed on the front face. At 41,000 lb, there was a sudden transverse failure across both scarf planks and the underlying structure. The out-of-plane deformations just prior to failure are shown in Fig. 11.

Test article CWA-1A behaved in a manner similar to test article CJA-2A. That is, inward facing half waves formed in all of the long spans near the tabs on both the front and back faces. At a load near 34,300 lb, the area around the impact damage began to move outward through a number of audible pops, until there was no longer an inward deflection, and an outward bulge of nearly 0.03 in. relative to the surrounding area formed. The front face in the vicinity of the impact damage also bulged outward, but over a larger area than on the back face and with an amplitude of approximately 10% of the back-face deformation. Catastrophic failure across the entire back face and across most of the front face occurred at 34,800 lb. The out-of-plane deformations just prior to failure are shown in Fig. 12.

The failure loads for the two impacted I-beam-joint test articles were significantly different with CWA-1A failing at a load 15% lower than that of CJA-2A. Test article CJA-2A failed at a load about 9% lower than the average of the pristine I-beam-joint test articles, and test article CWA-1A failed a load that was about 23% lower than the average of the pristine I-beam-joint test articles. Both impacted I-beam-joint test articles failed at loads higher by 10% or more than the impacted unjointed test articles. Similarly, the average failure strain for test article CWA-1A was 16% lower than that of CJA-2A. Test article CJA-2A had an average failure strain about 11% lower than the average of the pristine I-beam-joint test articles, and test article CWA-1A had an average failure strain that was about 32% lower than the average of the pristine I-beam-joint test articles. Both impacted I-beam-joint test articles had average failure strains equal to or higher the impacted unjointed test articles.

V. Concluding Remarks

Fluted-core composite structures have potential to provide benefits over traditional sandwich composites for certain aerospace applications. Fabrication of large autoclave-cured fluted-core cylindrical shells with existing autoclaves will require that the shells be fabricated in segments, and joined longitudinally to form a complete barrel. The experimental and computational study of the compression response of fluted core composite structures presented in Ref. 5 is extended in the current paper to experimentally investigate the compression behavior of basic and I-beam fluted-core-joint concepts. Both of these joint types had a scarf plank bonded over a scarfed region, and when compared with unjointed panels, the basic-joint test articles were only 11% stiffer and the I-beam-joint test articles were 22% stiffer. However, if the larger width of the I-beam-joint test articles is taken into account, the I-beam-joint test articles were less than 1% stiffer than the basic-joint test articles, and only 12% stiffer than the unjointed test articles. Pristine and impact-damaged test articles of both joint types were tested. Both buckling and strength failures were observed in the tested components. The stability response was manifested in plate-like local buckling patterns that were longitudinally distributed along individual flutes. Though these local-buckling events were not catastrophic by themselves, the deformations associated with the local buckling patterns may have led to material strength failures as loading was increased into the post-buckling range of loading. The pristine basic-joint test article performed well, by failing at a 13% higher load and a 22% higher average strain than the averages of the unjointed test articles. The pristine I-beam-joint test articles averaged 14% lower failure loads and 15% lower average strains than the averages of the unjointed test articles. The impacted basic-joint test article failed at a load 14% higher and an average strain 12% higher than the averages of the impacted unjointed test articles, and the I-beam-joint test articles failed at loads at least 10% higher and average failure stains equal to or higher than the averages of the impacted unjointed test articles. It is believed that the component flute size and facesheet thickness would also affect the influence of impacts on the load-carrying capability. Overall, for the test articles considered, both joint types added 11-12%, per unit width, to the unjointed longitudinal stiffness. When compared with the unjointed test articles, the failure loads of the basic-joint test articles scaled with this increase in longitudinal stiffness, but those of the I-beam-joint test articles did not. Therefore, it can be said that the basic-joint test articles performed similarly to the unjointed test articles and better than the I-beam-joint test articles.

Acknowledgments

This work was conducted as part of the NASA Engineering and Safety Center (NESC) Shell Buckling Knockdown Factor Project, NESC assessment number 07-010-E. All test articles discussed herein were produced and provided by The Boeing Company. Jeffrey Seebo of the Lockheed Martin Corp. at NASA Langley developed the system used for the ultrasonic scans and was instrumental in interpreting the data. The ultrasonic scans were performed by Richard Churray of NASA Langley.

References

- ¹Anonymous, "Ares I First Stage, Powering NASA's Newest Rocket," NASA Facts, FS-2008-05-86-MSFC.
- ²Anonymous, "NASA's Ares I Upper Stage, Powering the Second Phase of a Rocket's Journey to Space," NASA Facts, FS-2009-08-153-MSFC.
- ³Anonymous, "Constellation Program: America's Fleet of Next-Generation Launch Vehicles, The Ares V Cargo Launch Vehicle," NASA Facts, FS-2009-07-134-MSFC.
- ⁴Nettles, A. and Jackson, J., "Compression After Impact Testing of Sandwich Composites for Usage on Expendable Launch Vehicles," *Journal of Composite Materials*, Vol. 44, No. 6, 2010, pp. 707-738.
- ⁵Schultz, M.R., Oremont, L., Guzman, J.C., McCarville, D., Rose, C.A., Hilburger, M.W., "Compression Behavior of Fluted-Core Composite Panels," *Proceedings of the 52nd AIAA/ASME/ASCE/AHS/ASC Structures, Structural Dynamics, & Materials Conference*, AIAA paper no. 2011-2170, Denver, CO, April 2011.
- ⁶Campbell, F. C., *Manufacturing Processes for Advanced Composites*, Elsevier, New York, 2004.
- ⁷Thornburgh, R. P. and Hilburger, M. W., "Longitudinal Weld Land Buckling in Compression-Loaded Orthogrid Cylinders," NASA/TM-2010-216876, ARL-TR-5121, December 2010.
- ⁸VIC-3D, Software Package, Ver. 2010.1.0, Correlated Solutions, Inc., Columbia, SC, 2010.

Table 1: Experimental results for the unjointed and basic-joint test articles.






	CPA-1B, CPA-2B (pristine, average)	CPA-1A (impacted)	CPA-2A (impacted)	CJA-3B (pristine)	CJA-3A (impacted)
Joint type	None	None	None	Basic	Basic
Local buckling half-wave number(s)	9	7	None, 7, 9	9	None
Peak load, lb	52,500	30,900	31,700	59,200	35,800
Longitudinal stiffness, lb/in.	613,000	603,000	607,000	684,000	670,000
Average strain at failure, $\mu\epsilon$	7,300	4,500	4,600	8,900	5,100
Impact location	N/A	Short span 	Noodle 	N/A	Noodle 

Table 2: Experimental results for I-beam-joint test articles.

	CJA-2B (pristine)	CWA-1B (pristine)	CJA-2A (impacted)	CWA-1A (impacted)
Joint type	I-beam	I-beam	I-beam	I-beam
Local buckling half-wave number(s)	None	None, 9	None	None
Peak load, lb	42,300	47,600	41,000	34,800
Longitudinal stiffness, lb/in.	747,000	735,000	744,000	738,000
Average strain at failure, $\mu\epsilon$	5,900	6,500	5,500	4,600
Impact location	N/A	N/A	I-beam span 	I-beam noodle 

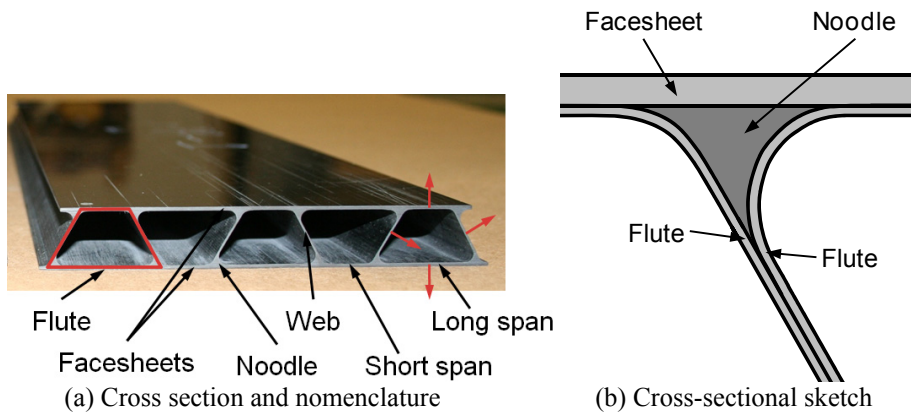


Figure 1. Cross section of an unjointed fluted-core composite panel.

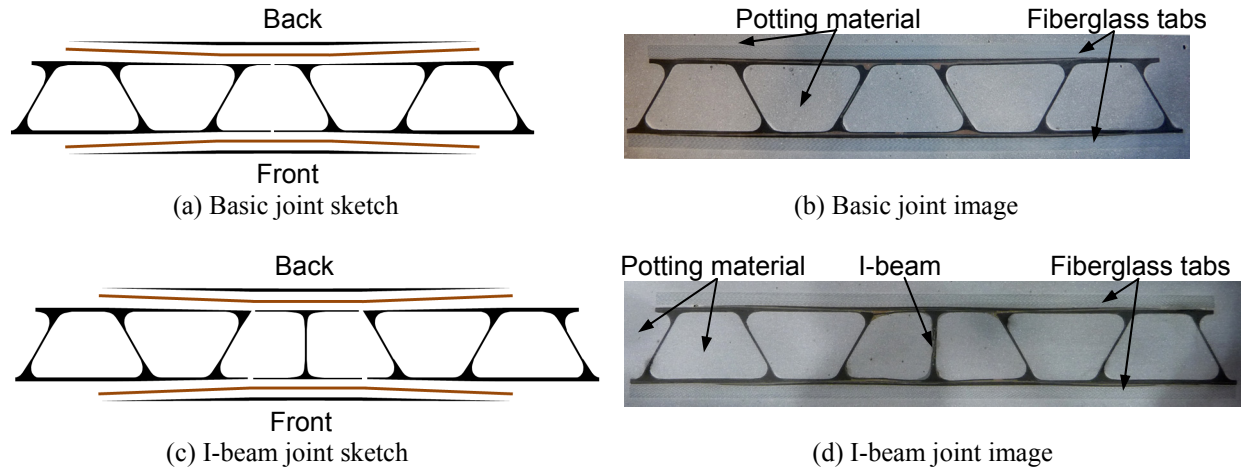


Figure 2. Joint configurations. The brown lines in (a) and (c) represent film adhesive.

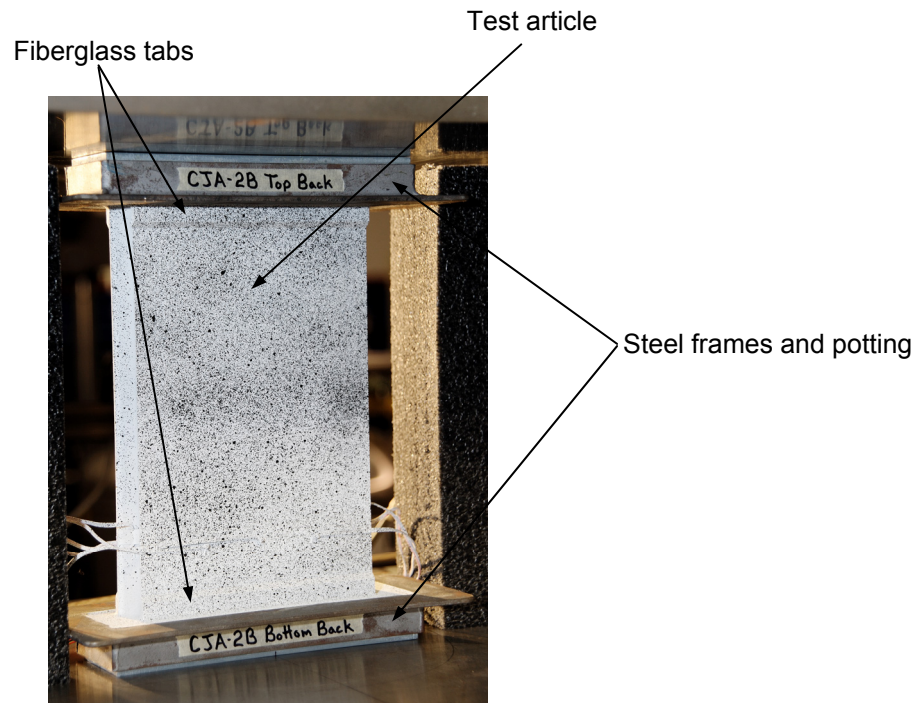


Figure 3. I-beam-jointed test article.

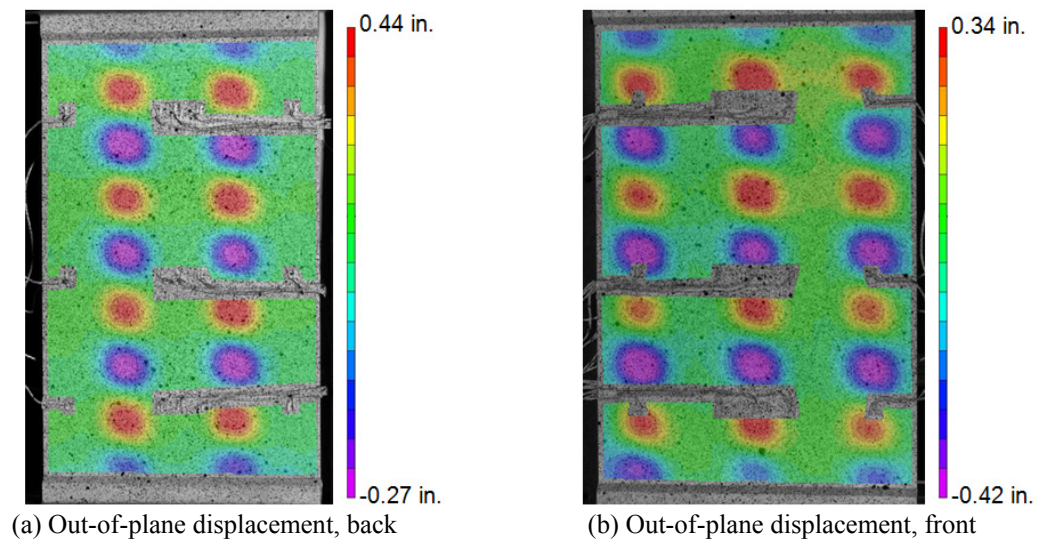


Figure 4. Local buckling pattern (out-of-plane displacement) in unjointed pristine test article (CPA-2B) with 53,500 lb compressive load. Positive displacements are outward.

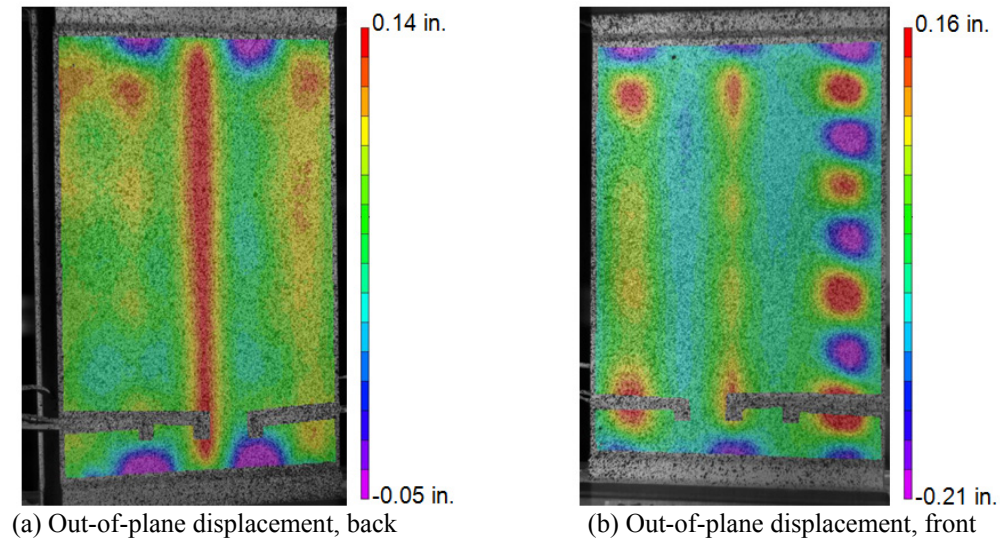


Figure 5. Test article CJA-3B (basic joint, pristine): 59,200 lb. Positive displacements are outward.

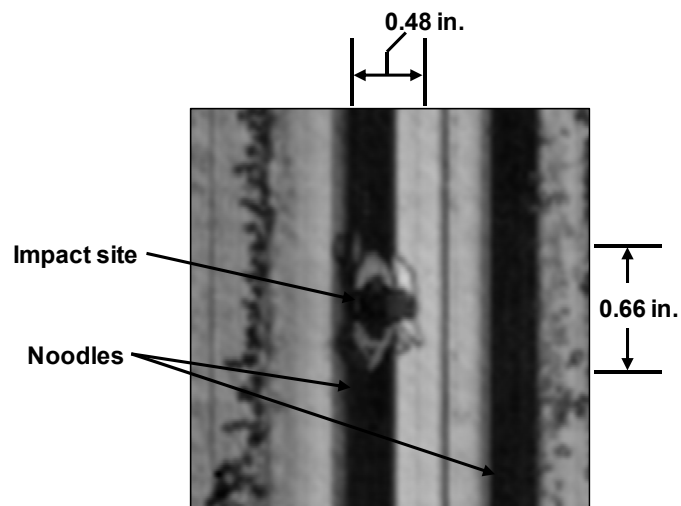


Figure 6. Ultrasonic scan of CJA-3A, the basic-joint test article with the over-noodle impact.

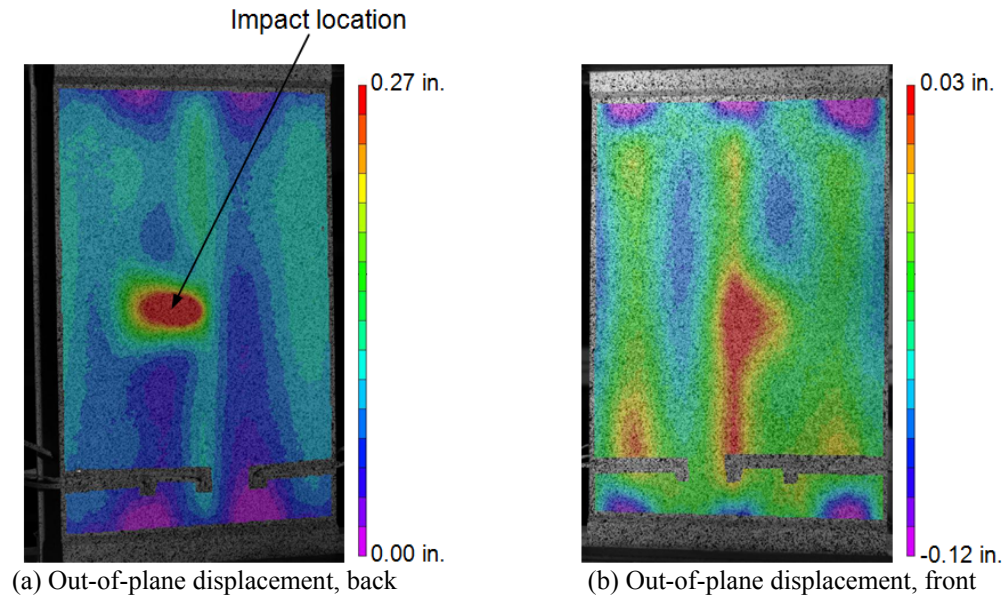


Figure 7. Test article CJA-3A (basic joint, backside noodle impact): 35,800 lb. Positive displacements are outward.

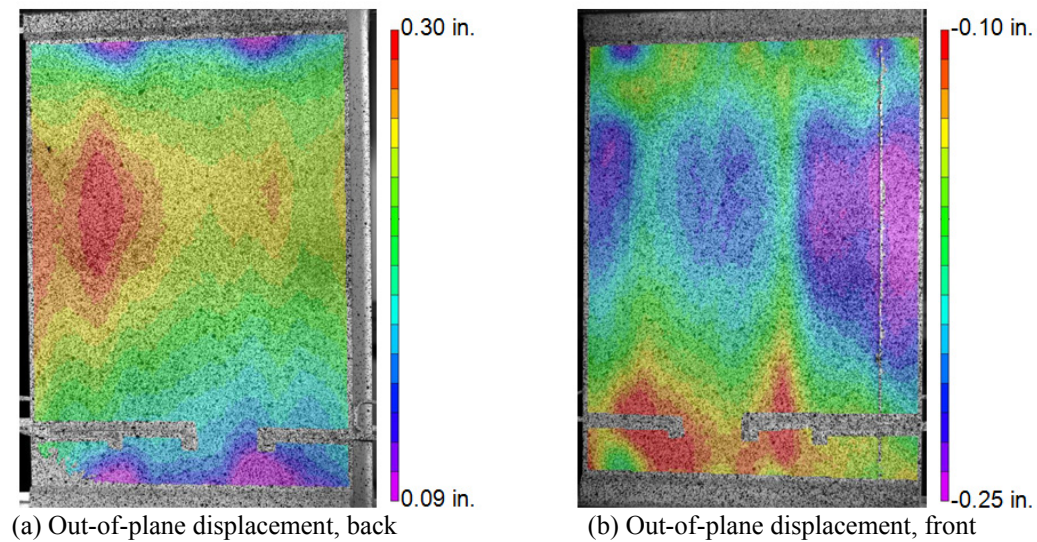


Figure 8. Test article CJA-2B (I-beam joint, pristine): 42,300 lb. Positive displacements are outward.

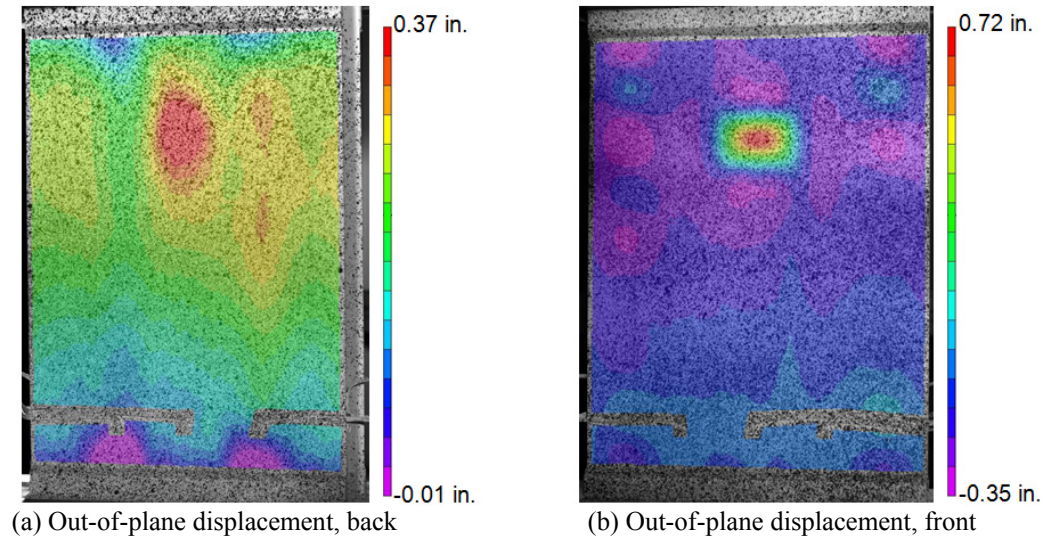


Figure 9. Test article CWA-1B (I-beam joint, pristine): 47,400 lb. Positive displacements are outward.

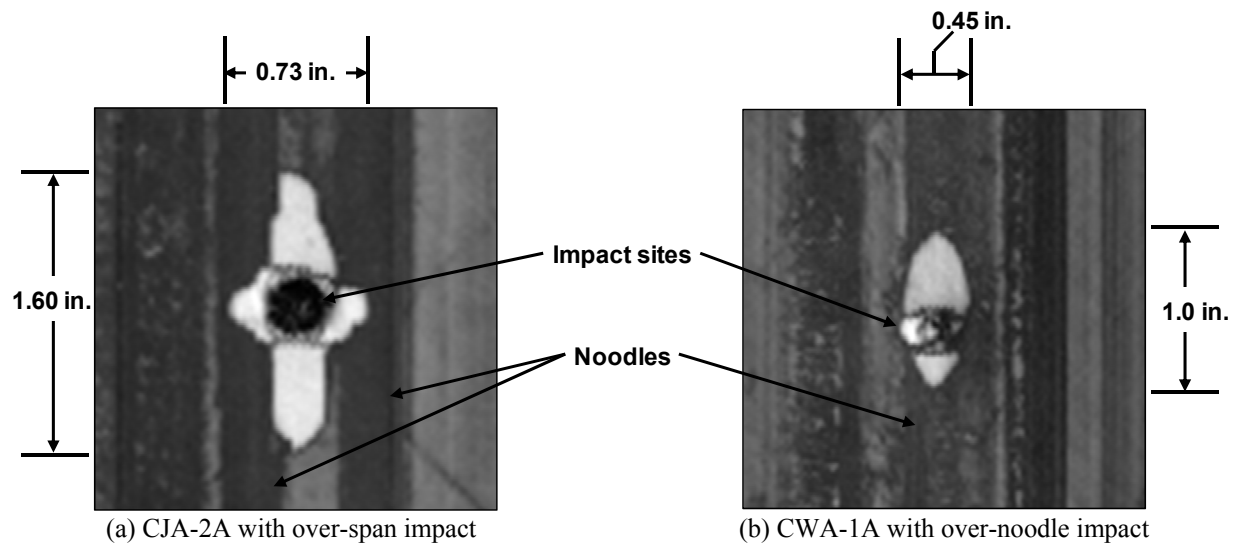


Figure 10. Ultrasonic scans of the impact regions of the impacted I-beam-joint test articles.

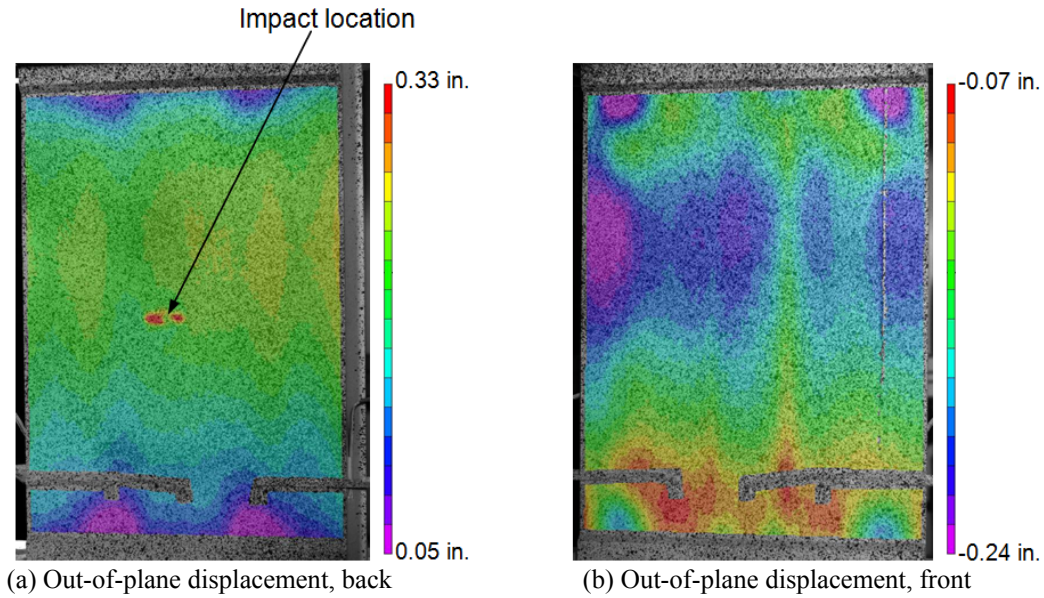


Figure 11. Test article CJA-2A (I-beam joint, backside impact between I-beam and noodle): 41,000 lb. Positive displacements are outward.

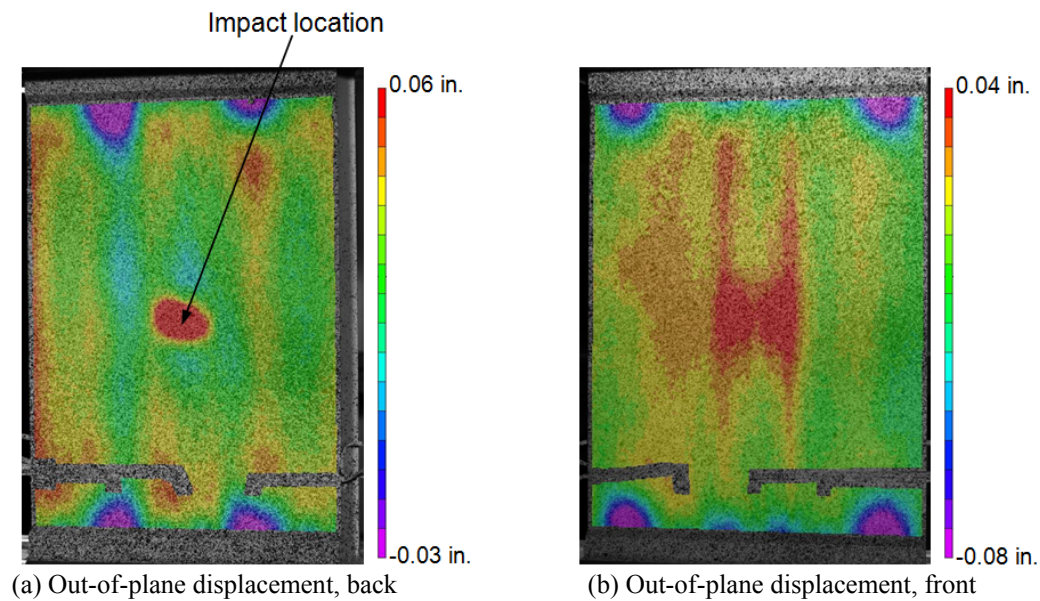


Figure 12. Test article CWA-1A (I-beam joint, backside I-beam noodle impact): 34,800 lb. Positive displacements are outward.